“VLT-SINFONI sub-kpc study of the star formation in local LIRGs and ULIRGs: Analysis of the global ΣSFR structure and characterisation of individual star-forming clumps”

López *et al.*, (2016) http://arxiv.org/abs/1603.03707 (A&A, accepted)

Abstract

We present a two-dimensional study of star formation at kiloparsec and sub-kiloparsec scales of a sample of local ($z < 0.1$) Luminous (10) and Ultraluminous (7) Infrared Galaxies (U/LIRGs), based on near-infrared VLT-SINFONI integral field spectroscopy (IFS). We obtained integrated measurements of the star formation rate and star formation rate surface density, together with their 2D distributions, based on Brγ and Paα emission. In agreement with previous studies, we observe a tight linear correlation between the star formation rate (SFR) derived from our extinction-corrected Paα measurements and that derived from *Spitzer* 24 μm data, and a reasonable agreement with SFR derived from L_{IR}. We also compared our $SFR_{Pa\alpha}$ values with optical measurements from Hα emission and find that the $SFR_{Pa\alpha}$ is on average a factor ~3 larger than the $SFR_{H\alpha}$, even when the extinction corrections are applied. Within the angular resolution and sizes sampled by the SINFONI observations, we found that LIRGs have a median-observed star formation rate surface density of $\Sigma^{obs}_{LIRGs} = 1.16\,M_\odot\,yr^{-1}\,kpc^{-2}$, and $\Sigma^{corr}_{LIRGs} = 1.72\,M_\odot\,yr^{-1}\,kpc^{-2}$ for the extinction-corrected distribution. The median-observed and the extinction-corrected Σ_{SFR} values for ULIRGs are $\Sigma^{obs}_{ULIRGs} = 0.16\,M_\odot\,yr^{-1}\,kpc^{-2}$ and $\Sigma^{corr}_{ULIRGs} = 0.23\,M_\odot\,yr^{-1}\,kpc^{-2}$, respectively. These median values for ULIRGs increase up to $1.38\,M_\odot\,yr^{-1}\,kpc^{-2}$ and $2.90\,M_\odot\,yr^{-1}\,kpc^{-2}$, when only their inner regions, covering the same size as the average FoV of LIRGs, are considered. For a given fixed angular sampling, our simulations show that the predicted median of the Σ_{SFR} distribution increases artificially with distance, a factor ~2-3 when the original measurements for LIRGs are simulated at the average distance of our ULIRGs. This could have consequences on any estimates of the star formation surface brightness in high-z galaxies, and consequently on the derivation of the universality of star formation laws at all redshifts.

We identified a total of 95 individual star-forming clumps in our sample of U/LIRGs, with sizes that range within ~60–400 pc and ~300–1500 pc, and extinction-corrected Paα luminosities of ~10^5–10^7 $L_\odot$ and ~10^6–10^8 $L_\odot$ in LIRGs and ULIRGs, respectively. The Σ_{SFR} of the clumps presents a wide range of values within 1–90 $M_\odot\,yr^{-1}\,kpc^{-2}$ and 0.1–100 $M_\odot\,yr^{-1}\,kpc^{-2}$ for LIRGs and ULIRGs. Star-forming clumps in LIRGs are about ten times larger and thousands of times more luminous than typical clumps in spiral galaxies, which is consistent with expected photon-bounded conditions in ionized nebulae that surround young stellar clusters. Clumps in ULIRGs have sizes similar (×0.5–1) to those of high-z clumps, having Paα luminosities similar to some high-z clumps, and about 10 times less luminous than the most luminous high-z clumps identified so far. This could be an indication that the most luminous giant clumps in high-z star-forming galaxies are forming stars with a higher surface density rate than low-z compact ULIRGs. We also observed a change in the slope of the L-r relation, from $\eta = 3.04$ of local samples to $\eta = 1.88$ from high-z observations. A likely explanation is that most luminous galaxies are interacting and merging, and therefore their size represents a combination of the distribution of the star-forming clumps within each galaxy in the system plus the additional effect of the projected distance between the galaxies. As a consequence, this produces an overall size that is larger than that of individual clumps, or galaxies (for integrated measurements)

近傍(z<0.1) のLIRG & ULIRGを近赤外面分光した論文の第3報

Paper 1 (2012)：天体カタログと輝線マップ

Paper 2 (2013)：各天体の減光マップと減光補正の議論

Paper 3 (this paper)：各天体のSFRとΣ_{SFR}の導出

【サンプル】

・親サンプル (Arribas 2008)： ~70天体

・面分光サンプル (Paper I) ：~ 17天体 (10 LIRG & 7 ULIRG)

【観測】

・SINFONI/VLT (2006 & 2008)

・ FoV 8” x 8” (FWHM ~0.63”)

・λ = 1.95–2.45 um, R ~ 3300,

	LIRG	ULIRG
Mean redshift	0.014	0.072
Mean Luminosity ($L/L_\odot$)	11.33	12.29
Covering size (kpc)	3 x 3	12 x 12
Spatial resolution (kpc)	0.2	0.9

サブkpcの空間分解能で星形成領域を分解

【結果】①星形成領域の空間分布

・減光補正したΣ_{SFR}は，median値が~50%増加．分布の幅も~50%広くなる

・Σ_{SFR} が LIRG > ULIRGなのは，前者の方が近いので外縁部(低Σ_{SFR})を観測していないことによるもの

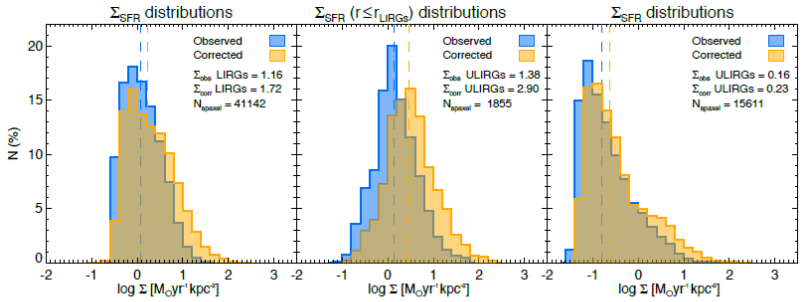

Fig. 6: Observed and extinction-corrected spaxel-by-spaxel Σ_{SFR} distributions of the LIRG subsample (left), of the inner spaxels ($r \le r_{LIRGs}$, see text for details) of the ULIRG subsample (centre), and the complete ULIRG distributions (right). The median Σ_{SFR} values and the total number of spaxels in each distribution are shown in the panels in units of $[M_\odot\,yr^{-1}\,kpc^{-2}]$ and plotted as dashed vertical lines.

② 星形成クランプの物理的性質

	LIRG	ULIRG
Size (pc)	60-400	300-1500
Luminosity ($L/L_\odot$)	10^5-7	10^6-8
Σ_{SFR} ($M_\odot$/ yr/ kpc²)	1-90	0.1-100

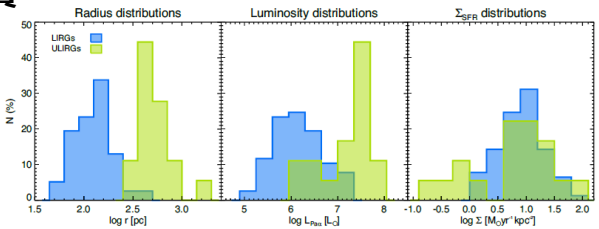

③ 近傍 & 遠方の星形成クランプとの比較

光度ー半径 のプロットの傾き η をみてやると，星形成領域の状態を推定可能．
(e.g. photon-bounded だとη=3)

・近傍U/LIRG
→ L(Paα) ~10^5を境に傾きが変化
(先行研究の示唆とconsistent)

・遠方U/LIRG
→ ULIRGはz~2のgiant clumpと同程度の光度をもつ

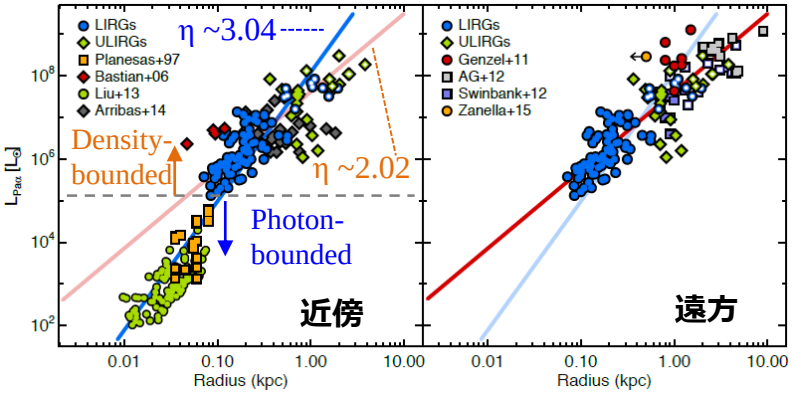

例：IRAS06206-6315 (Fig. 2B.2a)

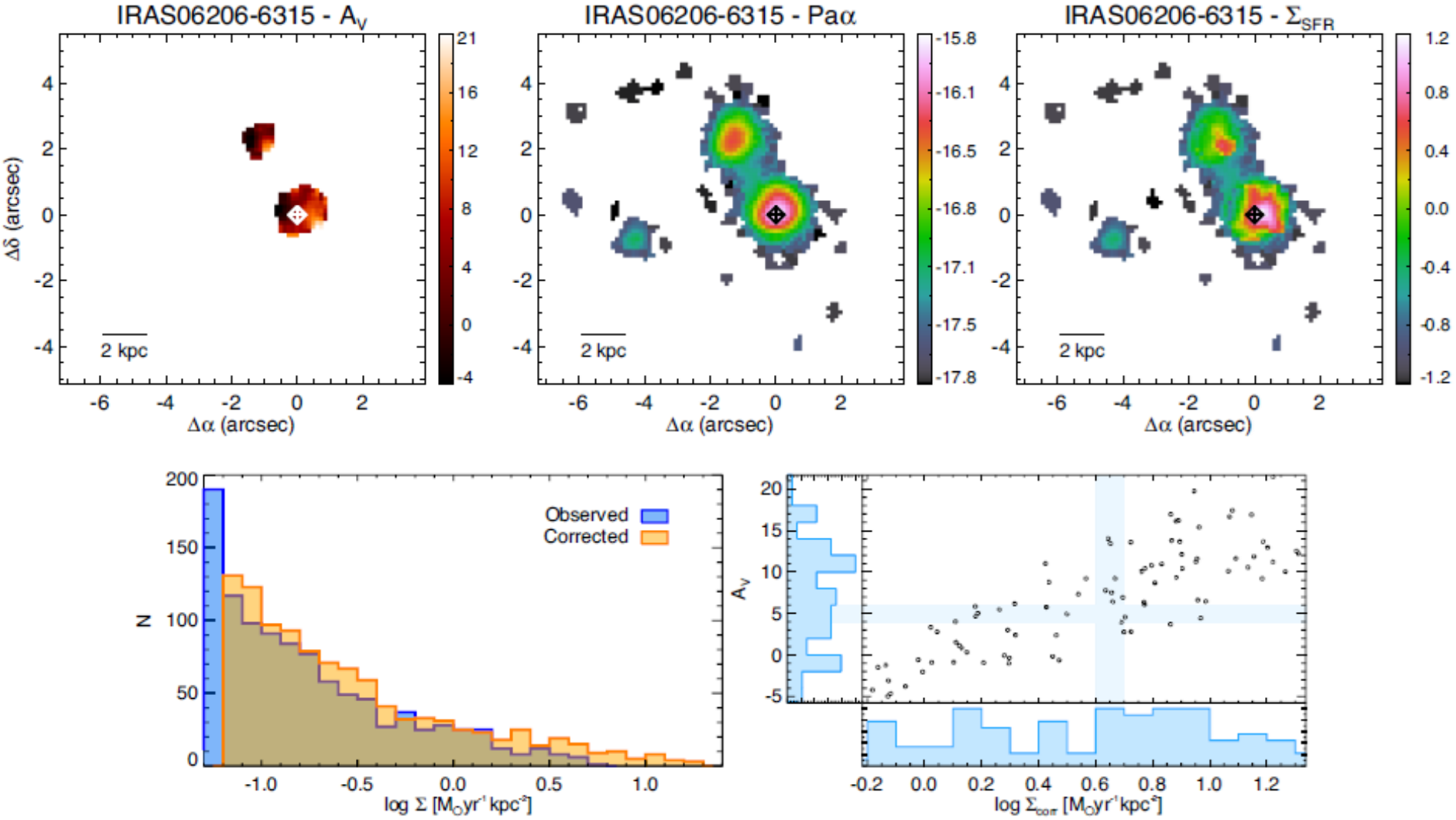

Fig. B.2a: IRAS 06206-6315. Top panels show the A_V map derived from the Paα at 1.876μm and Brγ at 2.166μm line ratio, the observed maps of the Paα emission, together with the star formation rate surface density (Σ_{SFR}) map, corrected from extinction. Units are [mag], log[erg s^{-1} cm^{-2}], and [$M_\odot$ yr^{-1} kpc^{-2}], respectively. The nucleus and Paα peak are marked with a plus sign (+) and a diamond ($\diamond$), respectively. The main nucleus is defined as the brightest spaxel of the SINFONI K-band image (Paper I), and the Brγ (Paα) peak corresponds to the brightest spaxel of the corresponding emission map. Bottom left panel shows the observed (blue histogram) and the corrected-from-extinction (yellow histogram) Σ_{SFR} spaxel-by-spaxel distributions. The relationship between the corrected Σ_{SFR} values and the A_V is shown in the bottom right panel only for those points with a spaxel-by-spaxel correction of the extinction. The blue histograms show the projected distribution onto each axis and are arbitrarily normalised, whereas the blue lines are the median of each distribution.